Effect of temperature and ARPC on powder concrete reinforcement

Amar Kumar Das[1], Bibhuti Bhusan Sahoo[2] and Abinash Samanta[3]

[1,3]Assistant Professor, Department of Mechanical Engineering, Gandhi Institute for Technology (GIFT), Bhubaneswar
[2]Assistant Professor, Department of Mechanical Engineering, Gandhi Engineering College, Bhubaneswar

Abstract: *The effects of high temperatures up to 800°C (1472°F) on portland- cement-based reactive powder concrete (CRPC) and alkali-acti- vated-slag-based reactive powder concrete (ARPC) were investi- gated within the scope of this study. The changes in the mechanical properties and microstructure of RPCs with elevated temperatures were evaluated. The test results indicated that CRPC has a supe- rior high temperature resistance up to 300°C (572°F) without any strength loss. Beyond this temperature, however, CRPC samples suffered from explosive spalling. Nevertheless, ARPC did not exhibit explosive spalling up to 800°C (1472°F) due to its nano-sized pored microstructure. These pores permit the quick escape of water vapor from the ARPC matrix, resulting in lower internal pore pressures. In conclusion, it can be said that the ARPC has a better high tempera- ture resistance compared to the conventional RPC.*

Keywords: alkali-activated cement; high temperature; mechanical properties; microstructure; reactive powder concrete; spalling.

INTRODUCTION

High-performance concretes (HPCs) with high strength or durability properties have been gradually replacing normal-strength concrete, especially in structures exposed to severe loading and environmental conditions. The advantages of HPC are the result of improvement of the internal structure, which is denser than normal concrete. However, this dense microstructure of HPC seems to be a disadvantage in the case of fire.[1-3] Following the first fire that occurred in an HPC structure—the Channel tunnel fire—and from different studies in progress, it is clear that the fire resistance of HPC does not seem to be as good as that of ordinary concrete.[4] It was observed that HPC is susceptible to spalling or even explosive spalling when subject to rapid temperature rise.[1,5,6] Severe damages with spalling in HPC structures densified by silica fume, such as the Great Belt tunnel in Denmark and the Channel tunnel, have been reported.[4,7] In light of this information, it is obvious that this portrait will be more pessimistic for ultra-high-performance concretes such as reactive powder concrete (RPC).

RPC is a relatively new cement-based ultra-high-performance composite developed through microstructural engineering. Conventional RPC is composed of portland cement and ultra-fine powders, such as crushed quartz and silica fume; it also has a low water content (water-cementitious material ratio [*w*/*cm*] generally lower than 0.20). The dense matrix is achieved by optimizing the granular packing of these powders.[8] The mechanical properties that can be achieved include compressive strength between 200 and 800 MPa (29 and 115.9 ksi), fracture energy between 1200 and 40,000 J/m^2 (1200 and 40,000 N/m), and ultimate tensile strain on the order of 1%.[8,9] This is generally achieved by a microstructural design approach, including elimination of the coarse aggregates, reducing the *w*/*cm*, lowering the CaO/SiO_2 ratio by introducing silica components, and the incorporation of steel microfibers.[8-10] However, the absence of voids, which relieves the internal thermal stresses, creates a major problem in the case of fire.

Hertz[7] classified the dense concretes into two classes: dense and super dense. According to this classification, conventional portland-cement-based RPC (CRPC) belongs to the super-dense concrete class. For super-dense concrete, crystal water may be sufficient enough for causing an explosive spalling without any external or thermal stresses. However, dense concretes need thermal and external stress causes to exhibit spalling damages. Also, according to Hertz's theory,[7] polypropylene fibers do not prevent spalling of super-dense concretes or in constructions such as drilled tunnels, where thermal curvature is hindered. Besides, using polypropylene fibers in RPC production also creates some problems, such as workability and strength reduction. Thus, the performance of RPC under high temperature seems to be a considerable handicap for its application. However, composites with similar properties to conventional RPC can also be produced by the activation of slag and silica fume (SF).[11] The microstructure of this composite includes a countless number of nano-pores and it is significantly different from conventional RPC. This unique microstructure may be a solution for the explosive spalling behavior of ultra-high-strength concretes.

RESEARCH SIGNIFICANCE

Studies on RPC have increased substantially within the last decades due to its superior mechanical properties. The super-dense microstructure of this composite provides good durability in severe exposure conditions. However, this dense microstructure of RPC seems to be a disadvantage in the case of fire. An alternative composite, alkali-activated-slag-based RPC (ARPC), has been developed in the Dokuz Eylul University Construction Laboratory with similar mechanical properties and a very different microstructure compared to CRPC. The developed ARPC is composed of nano-pores. Thus, it may be a good alternative in the case of fire. In the scope of this paper, the high temperature resistance of conventional CRPC and ARPC was comparatively evaluated.

EXPERIMENTAL INVESTIGATION

ARPC was developed in the Dokuz Eylul University Construction Materials Laboratory as a result of many experimental studies.[11] Following the development of ARPC, this

study was implemented to determine the high temperature resistance of this composite in comparison with the conventional CRPC with similar mechanical properties.

Materials

Ground-granulated blast-furnace slag (GGBFS) was procured from the Ereğli steel plant in Turkey. The chemical composition of GGBFS is presented in Table 1. The specific gravity and specific surface (Blaine) values of GGBFS were 2.88 and 410 m^2/kg, respectively. It contained 90% particles sized smaller than 45 µm. It was neutral with the basicity coefficient (K_b = (CaO + MgO)/(SiO_2 + Al_2O_3)) of 0.81. As can be seen from Table 1, the hydration modulus (HM = (CaO + MgO + Al_2O_3)/SiO_2) of slag was 1.33.

CEM I 42.5 ordinary portland cement (PC) with a 369 m^2/kg Blaine fineness was used in the production of CRPC. A commercial SF was also used in this study with the chemical composition seen in Table 1. The specific surface area and specific gravity of SF were 23,360 m^2/kg (114,230.4 ft^2/lb) (Brunauer-Emmett-Teller [BET] nitrogen adsorption method) and 2.20, respectively.

ARPC was produced by the activation of GGBFS and SF with the mixture of technical-grade sodium hydroxide and sodium silicate providing silicate modulus (M_S = SiO_2/Na_2O) in the solution 1.2 and Na_2O 4% by weight of the binder. The activator solution was prepared 1 day before casting.

A polycarboxylate-based high-range water-reducing admixture complying with ASTM C494/C494M-08,[12] Type F, and TS EN 934-2[13] was used in the production of CRPC. The specific gravity and solid content of the high-range water-reducing admixture were 1.06 and 40%, respectively.

Brass-coated steel fibers 13 mm (0.512 in.) in length and 0.16 mm (0.0063 in.) in diameter were used. The aspect ratio and tensile strength of this fiber were 81.25 and 2250 MPa (11.78 and 304.3 ksi), respectively.

A commercial quartz sand in four different size fractions (1 to 3 mm [0.0394 to 0.12 in.], 0.6 to 1.2 mm [0.024 to 0.05 in.], 0 to 400 µm, and 0 to 75 µm), was used as aggregate.

Specimens

Prismatic specimens (40 x 40 x 160 mm [1.57 x 1.57 x 6.30 in.]) were subjected to high temperatures. Mechanical properties, such as flexural strength and toughness, were measured on these prismatic specimens. The two broken pieces left from the flexural test were subjected to the compressive strength test.

Items of investigation

The mixture designs of ARPC and CRPC are presented in Table 2. The steel fiber volume was 1.5% in both series. Also, most of the other design parameters of these mixtures were kept similar, such as total binder, SF and aggregate contents, water-binder ratio (*w*/*b*), and so on.

Table 1—Chemical compositions (%) of GGBFS, PC, and SF

	SiO_2	Fe_2O_3	Al_2O_3	CaO	MgO	Na_2O	K_2O	SO_3	Loss on ignition
GGBFS	40.20	1.68	11.66	35.90	5.88	0.30	1.47	0.90	0.88
PC	19.10	3.96	4.40	61.85	2.05	0.27	0.70	3.72	1.82
SF	96.10	—	—	—	—	—	—	—	1.81

Table 2—Mixture designs for ARPC and CRPC

	ARPC	CRPC
GGBFS, kg/m^3 (lb/yd^3)	720.0 (1213.6)	—
PC, kg/m^3 (lb/yd^3)	—	720.0 (1213.6)
SF, kg/m^3 (lb/yd^3)	180.0 (303.4)	180.0 (303.4)
Quartz (1 to 3 mm [0.0394 to 0.12 in.]), kg/m^3 (lb/yd^3)	543.2 (915.6)	575.3 (969.7)
Quartz (0.6 to 1.2 mm [0.024 to 0.05 in.]), kg/m^3 (lb/yd^3)	422.5 (712.1)	447.5 (754.3)
Quartz (0 to 400 µm), kg/m^3 (lb/yd^3)	144.9 (244.2)	153.4 (258.6)
Quartz (0 to 75 µm), kg/m^3 (lb/yd^3)	96.6 (162.8)	102.3 (172.4)
Steel fiber, kg/m^3 (lb/yd^3)	117.8 (198.6)	117.8 (198.6)
Waterglass, kg/m^3 (lb/yd^3)	160.0 (269.7)	—
NaOH, kg/m^3 (lb/yd^3)	30.9 (52.1)	—
Water, kg/m^3 (lb/yd^3)	49.0 (82.6)	123.0 (207.3)
High-range water-reducing admixture, kg/m^3 (lb/yd^3)	—	50.0 (84.3)
Unit weight, kg/m^3 (lb/yd^3)	2465 (4154.8)	2469 (4161.6)
w/*b*	0.17	0.17
Aggregate-binder ratio	1.34	1.42

In the preparation of ARPC, the powders were dry-mixed at a low speed (99 rpm) in a pan-type specially designed mixer for approximately 1 minute. After the introduction of activator solution, the materials were mixed at a low speed (99 rpm) for 1 minute, then at a high speed (440 rpm) for approximately 2 minutes. In the second stage, aggregates were added to a premixed composition and mixed at the same high speed for approximately 2 minutes. Finally, steel fibers were added to the mixture and remixed for 3 to 4 minutes at a high speed to achieve a uniform fiber dispersion. A similar procedure was applied for the production of CRPC samples. The mixtures were cast into molds and compacted by hand operations and vibration. The specimens were kept in the molds for 5 hours at a room temperature of approximately 20°C (68°F) and were exposed to steam curing at 100°C (212°F) for 12 hours at a heating rate of 22°C/h (71.6°F/h). Then, the prisms were kept in laboratory conditions (approximately 20°C [68°F] and 55% relative humidity) for 2 days before testing. The long-term strength of steam-cured concrete is of lesser importance for many applications because its rate of strength development is considerably high and these products generally can be handled soon after casting.[14] Thus, the long-term strength of steam-cured RPC was not a major property to be determined.

Two days after the curing period, three prismatic specimens from each mixture were exposed to 200, 300, 400, 600, and 800°C (392, 572, 752, 1112, and 1472°F) temperatures for 3 hours in the oven. The heating rate was 10°C/minute (50°F/minute). The hot mortar specimens were slowly cooled in the laboratory conditions. At the end of the cooling period, the prismatic specimens were subjected to the flexural strength test.

The flexural test specimens were tested at a loading rate of 0.2 mm/minute (0.0078 in./minute) up to a midspan deflection of 3 mm (0.12 in.) under a closed-loop control test procedure. The specimens were loaded from their midspan and the clear distance between the simple supports was 130 mm (5.12 in.). The toughness was regarded as the area under the load-deflection curve up to a 3 mm (0.12 in.) midspan deflection. The two broken pieces left from the flexural test were subjected to the compressive strength test. The flexural strength, compressive strength, and toughness test results were compared with the test results of the control specimens that were not exposed to high temperatures. Each datum presented is the average test results of at least three specimens for the flexural strength and toughness tests and at least six specimens for the compressive strength tests. Scanning electron microscope (SEM) and porosimetry analyses were implemented on the middle portion of samples taken from the inner part of the mortar specimens (approximately 10 mm [0.394 in.] from the surface).

The microstructures of both RPC mixtures were investigated by using an SEM. The samples for SEM analysis were prepared by taking small pieces from the prismatic specimens. The original microstructure and morphology of the RPCs were observed on the fractured surfaces by secondary electron imaging. The general microstructural features of RPC samples were also determined by using backscattered electron (BSE) imaging. The basic principles of the BSE imaging process of the cementitious microstructures were explained by Scrivener[15] and Diamond.[16] The pore-size distributions of the samples were determined by the mercury intrusion porosimetry (MIP) method. Thermogravimetric (TG) analyses were applied on oven-dried powder samples taken from the inner part of the specimens. The sample was heated in an inert nitrogen environment at 10°C/minute (50°F/minute) up to 1000°C (1832°F). The TG and differential thermal analysis (DTA) (TG/DTA) and derivative thermogravimetric curve (DTG) were used to evaluate the thermal effects on RPC samples.

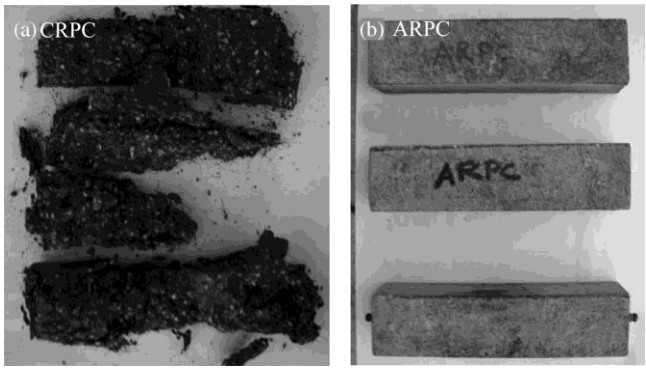

Fig. 1—CRPC and ARPC specimens after exposure to 600°C (1112°F).

EXPERIMENTAL RESULTS AND DISCUSSION

In this study, two different types of RPC samples were subjected to high temperatures up to 800°C (1472°F). However, CRPC specimens suffered explosive spalling when the temperature reached 450°C (842°F) or after exposure to 400°C (752°F) for 18 minutes (Fig. 1). Thus, the residual mechanical properties for CRPC could be evaluated up to 300°C (572°F). In contrast to CRPC, however, ARPC specimens were resistant to high temperatures up to 800°C (1472°F).

The risk of explosive spalling increases with a high heating rate.[17-19] To display the degree of explosive spalling resistance of ARPC, ARPC specimens were also heated by a higher heating rate of 25°C/minute (77°F/minute) up to 800°C (1472°F). None of the ARPC specimens exploded up to 800°C (1472°F), even at this high heating rate. Shi et al.[20] stated that there is a higher risk of explosive spalling for alkali-activated cement concrete when exposed to high temperatures due to its low capillary porosity. However, the test results for ARPC show that the explosive spalling behavior of alkali-activated cements is strongly related to its composition. The results of this study also indicate that the risk of explosive spalling for GGBFS/SF-based ARPCs is significantly lower than the conventional RPCs that have a similar composition and mechanical properties.

Weight and length change

The weight loss and length change of specimens due to the high temperature exposure are presented in Table 3. Weight losses increased with the increase of temperature as expected. The loss of cementitious components below 400°C (752°F) is negligible for portland-cement-based materials.[3] The mass loss is mainly associated with the water loss—transferred outward in a vapor state. The ARPC samples showed a higher weight loss than CRPC samples up to 300°C (572°F), possibly due to the higher moisture content and porosity of ARPC. On the other hand, both RPC samples showed shrinkage behavior at 200°C (392°F). However, shrinkage of ARPC is significantly higher than CRPC, as parallel to the weight loss. Shrinkage behavior

Table 3—Weight loss and length change of ARPC and CRPC

	Weight loss, %				
	200°C (392°F)	300°C (572°F)	400°C (752°F)	600°C (1112°F)	800°C (1472°F)
ARPC	4.4	5.8	6.1	6.3	6.3
CRPC	0.8	4.5	—	—	—

	Length change, %			
	200°C (392°F)	400°C (752°F)	600°C (1112°F)	800°C (1472°F)
ARPC	–0.14	–0.08	+0.27	+6.31
CRPC	–0.02	—	—	—

Table 4—Mechanical properties of ARPC and CRPC

	ARPC	CRPC
Compressive strength, MPa (ksi)	215.9 (31.3)	214.6 (31.1)
Flexural strength, MPa (ksi)	41.5 (6.0)	34.7 (5.0)
Toughness, N.mm (lb.in.)	25,341 (224.3)	22,307 (197.4)

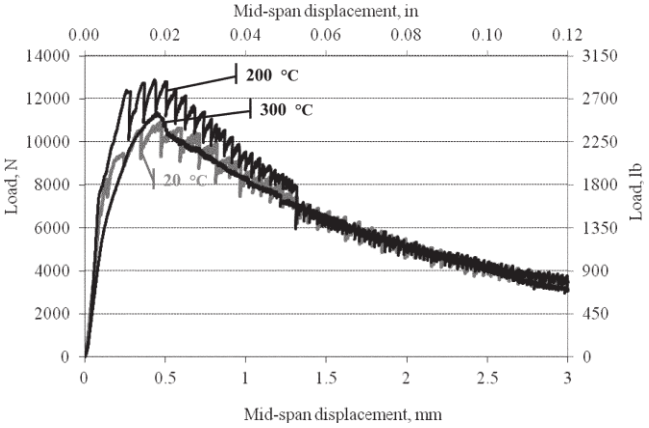

Fig. 2—Load-displacement curves of CRPC versus temperatures. (Note: °C = (°F – 32)/1.8.)

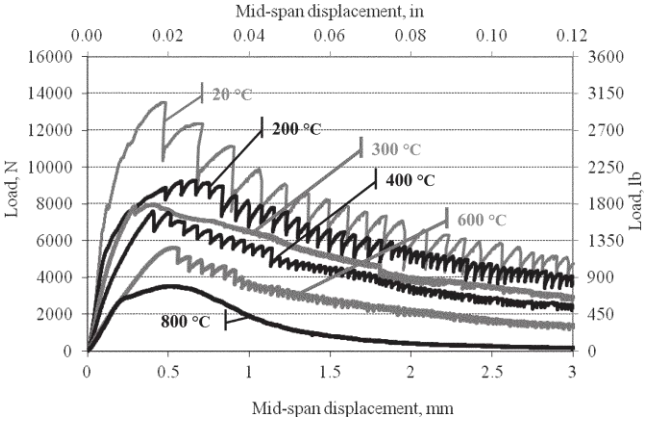

Fig. 3—Load-displacement curves of ARPC versus temperatures. (Note: °C = (°F – 32)/1.8.)

continued for ARPC samples up to 400°C (752°F). However, ARPC started to expand from 600°C (1112°F) and up. When the temperature was elevated to 800°C (1472°F), the expansion level of ARPC reached critical values that can threaten the structural integrity. The expansion at 600°C (1112°F) is somewhat related to the quartz aggregate used in the RPC compositions. Siliceous aggregates containing quartz may cause distress in concrete at approximately 573°C (1063°F) because the transformation of quartz from α to β form is associated with a sudden expansion of the order of 0.85%.[21] However, expansion at 800°C (1472°F) is not only related to quartz transformation. It is also related to the matrix phase of ARPC. Prismatic 40 x 40 x 160 mm (1.57 x 1.57 x 6.30 in.) ARPC paste specimens were subjected to 800°C (1472°F) for 3 hours to investigate this phenomenon, and the expansion of the ARPC matrix phase was found to be 14.6% higher than the ARPC composite.

Load-displacement curves

The load-versus-midspan deflection curves of CRPC samples for various temperatures up to 300°C (572°F) are presented in Fig. 2. At all temperatures, CRPC presented deflection-hardening behavior that generates a higher load-carrying capacity after the first cracking. The load-carrying capacities of samples increased with the increase of temperature. Greater load-carrying capacity after the peak load indicates improvement in toughness and the reinforcing effect of steel fibers. Sudden load drops were observed in the descending branch up to 200°C (392°F). This behavior was not observed at 300°C (572°F). This behavior may be attributed to the reduced matrix-fiber bond effect at 300°C (572°F).

The load-versus-midspan deflection curves for ARPC samples for various temperatures up to 800°C (1472°F) are presented in Fig. 3. Similar to CRPC, ARPC samples also presented a deflection-hardening behavior at all temperatures. However, the load-carrying capacity of ARPC samples decreased steadily with the increase of temperature. Sudden load drops were not observed in the descending branch for 800°C (1472°F), possibly due to the loss of bond between matrix fibers.

Mechanical properties

The mechanical properties of ARPC and CRPC samples before exposure to high temperatures are given in Table 4. As shown in Table 4, ARPC and CRPC samples have a similar compressive strength value of approximately 215 MPa (31 ksi), whereas the flexural strength and toughness values of ARPC are 19.6% and 13.6% higher than CRPC, respectively.

The relative residual compressive strength, flexural strength, and toughness values of CRPC after exposure to high temperatures are also presented in Fig. 4. The relative residual values of mechanical properties represent the ratio between the mechanical properties of exposed specimens and control specimens. The residual compressive and flexural strength values of CRPC increased up to 300°C (572°F). The compressive and flexural strengths of CRPC at 300°C (572°F) reached 279 and 40.3 MPa (40.4 and 5.8 ksi), respectively. However, the mechanical properties of CRPC could not be determined beyond 400°C (752°F) due to the damage of the samples. This behavior can be attributed to the super-dense microstructure of this composite, which appeared as a result of a low *w*/*cm* and high SF content. Tai et al.[22] also reported that RPC is highly prone to spalling within a temperature range of 400 to 500°C (752 to 932°F) at high heating rates. Besides, test results indicated that the compressive strength of RPC increased with a temperature up to 300°C (572°F) and then decreased sharply.[22] Similar

results were also reported by Hertz.[23] The strength gain up to 300°C (572°F) may be due to the relief of pressures by drying, which also creates greater Van der Walls forces, resulting in a closer configuration of capillary pores.[24,25] The toughness of CRPC at 200°C (392°F) increased by 16%, whereas a slight reduction in toughness appeared at 300°C (572°F). The increase of fracture energy for steel fiber-reinforced HPC with the increase of temperature to 400°C (752°F) was also reported by Peng et al.[26] This improvement for fracture energy, explained by a more pronounced fiber pullout process, could take place during the fracture of fiber-reinforced concrete after heating. Another possible reason for the increase in fracture energy after heating might be the interlocking of aggregates during the fracture process, according to Peng et al.[26]

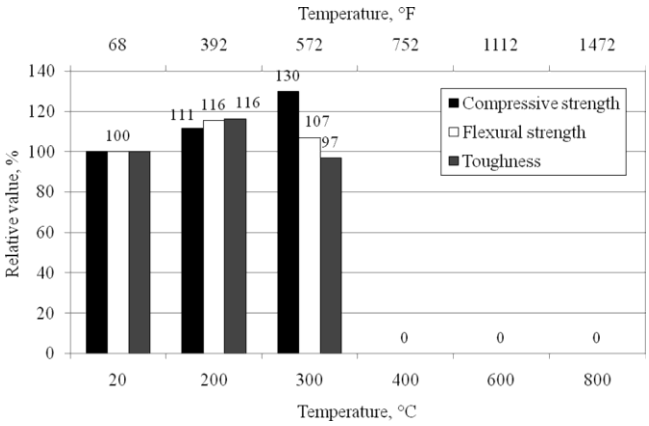

Fig. 4—Relative mechanical properties of CRPC versus temperatures.

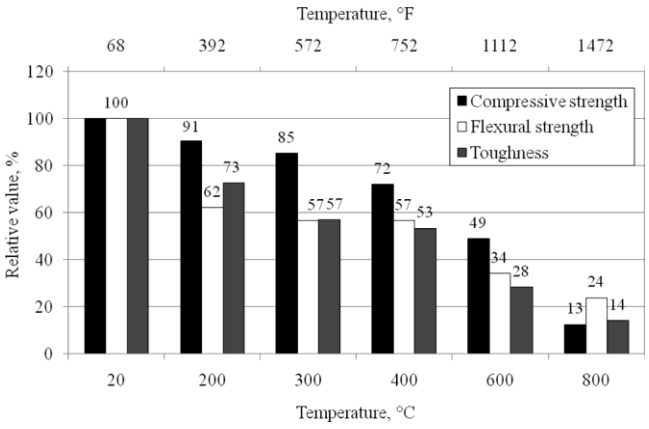

Fig. 5—Relative mechanical properties of ARPC versus temperatures.

Hertz[17] concluded that portland cement concretes densified by means of SF at high moisture contents are more likely to explode and suggested an upper limit of 10% by weight of cement on silica fume to avoid spalling. This limit was proposed as 5% by Poon et al.[6] Both CRPC and ARPC compositions contained 20% SF. Nevertheless, none of the ARPC specimens exploded up to 800°C (1472°F). In other words, these limits do not seem to be valid for alkali-activated slag/SF ultra-high-strength concrete, according to the results of this study.

The relative residual mechanical properties of ARPC samples are presented in Fig. 5. All of the mechanical properties of ARPC samples decreased parallel to the increase of temperature, even at a relatively low temperature of 200°C (392°F). Nevertheless, the residual compressive and flexural strengths of ARPC at 600°C (1112°F) were 105.8 and 11.8 MPa (15.3 and 1.7 ksi), respectively. ARPC samples were durable to high temperatures and with these residual strength values, they still can be classified as ultra-high-strength concrete. The maximum reduction ratios in the mechanical properties were generally observed in the toughness values. The reduction was followed by flexural and compressive strengths, respectively. ARPC compositions seem to promise high-performance material for the structures with the high fire risk.

With respect to high temperature resistance, the best performance was generally recorded for slag-incorporated portland-cement concrete compared to fly ash and SF concretes.[27,28] Diederichs et al.[28] showed that slag incorporating high-strength concretes (HSCs) has the best high temperature performance, followed by fly ash and SF concretes.

Microstructure investigation

SEM and MIP analyses were planned to analyze the variation in the microstructure of the mixtures after exposure to high temperatures. These analyses were realized on CRPC samples for 20 and 300°C (68 and 572°F) and ARPC samples for 20, 200, and 600°C (68, 392, and 572°F).

Figure 6 shows the SEM (BSE) images of CRPC samples for 20 and 300°C (68 and 572°F). Before its exposure to high temperature, the CRPC matrix contains several microcracks—possibly due to the high cement content of this mixture that generates shrinkage strains in the matrix. After exposure to a temperature of 300°C (572°F), these

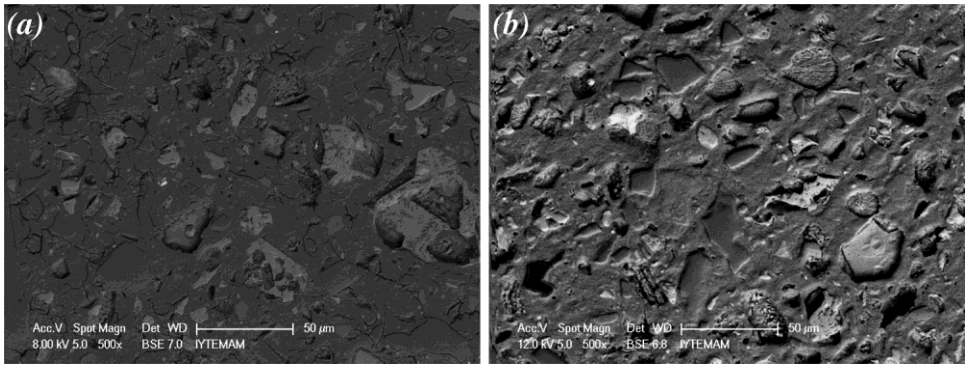

Fig. 6—SEM (BSE) image of CRPC: (a) 20°C (68°F); and (b) 300°C (572°F).

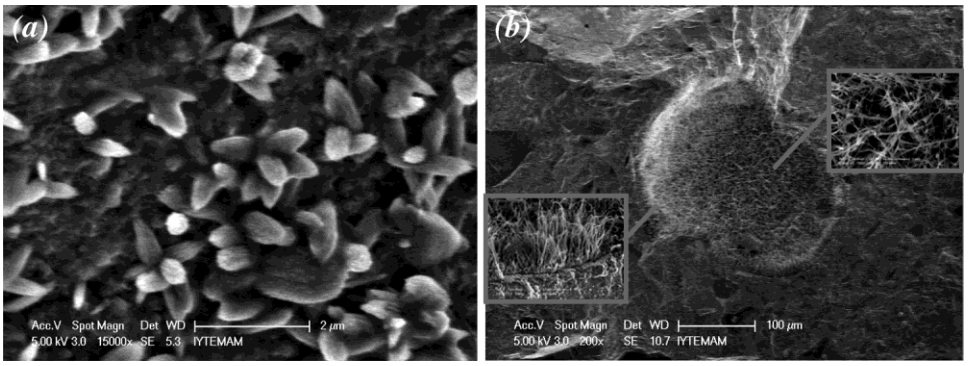

Fig. 7—SEM (SE) image of CRPC: (a) 20°C (68°F); and (b) 300°C (572°F).

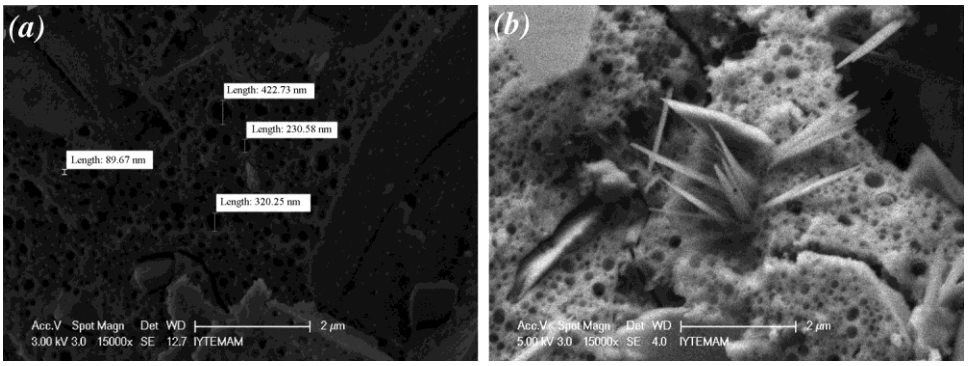

Fig. 8—SEM (SE) image of ARPC: (a) 20°C (68°F); and (b) 200°C (392°F).

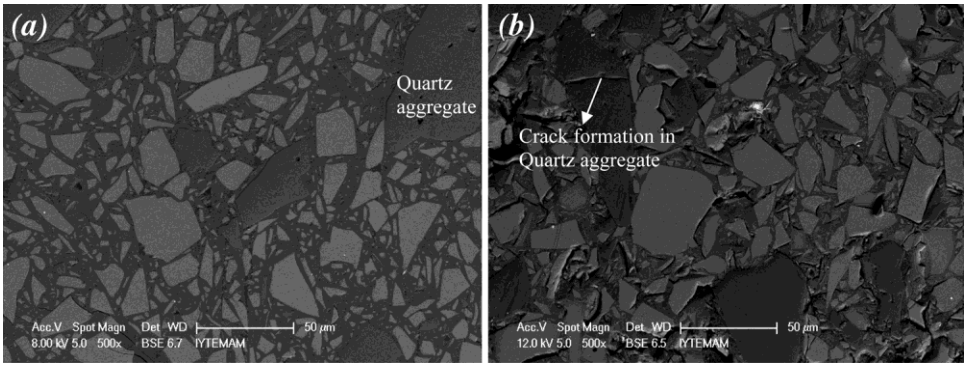

Fig. 9—SEM (BSE) image of ARPC: (a) 20°C (68°F); and (b) 600°C (1112°F).

cracks disappeared. This phenomenon might be due to the continued hydration of the matrix under the presence of water and temperature and closer configuration of the matrix parallel to the evaporation of capillary water. This healing in the microstructure may be the main reason for the strength increase at this temperature. Figure 7 shows the SEM (SE) images of CRPC for 20 and 300°C (68 and 572°F). It can be seen that spherical pores have been partially filled with needle-like tobermorite formations after exposure to 300°C (572°F). Energy-dispersive spectroscopy (EDS) analysis showed that Ca/Si, S/Ca, and Al/Ca ratios of this type of tobermorite were 1.03, 0.011, and 0.11, respectively.

SEM (SE) images of ARPC samples at 20 and 200°C (6 and 572°F) are presented in Fig. 8. The most important difference of ARPC to CRPC is the existence of a great number of nano-pores in the ARPC matrix (Fig. 7(a) and 8(a)). These pores may be the reason for the nonexplosive spalling behavior of ARPC. These pores permit the quick escape of water vapor from the ARPC matrix, resulting in lower internal pore pressures. Thus, ARPC does not suffer explosive spalling, whereas CRPC exhibits serious damage. Needle-like formations appeared when the temperature rose to 200°C (392°F) (Fig. 8(b)). The strength losses at 200°C (392°F) possibly arise from the stresses created by the needle-like formations in the ARPC matrix. The SEM (BSE) image of ARPC subjected to 600°C (1112°F) is shown in Fig. 9 with the unheated situation. The deterioration observed in the aggregate-matrix transition zone and the crack formations in the quartz aggregate due to the transformation of α quartz to β quartz are the main differences compared to the unheated case. Cracks were also observed in the matrix phase of ARPC at this temperature level.

The TG curves of CRPC and ARPC are shown in Fig. 10 and 11, respectively. DTA shows the ranges corresponding to different phases in the paste, while simultaneous weight loss due to decomposition is estimated with

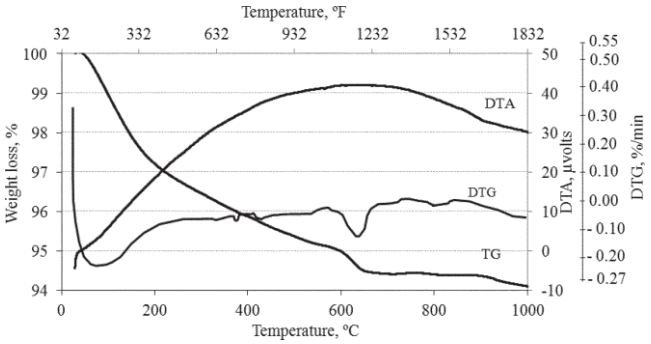

Fig. 10—TG curve of CRPC.

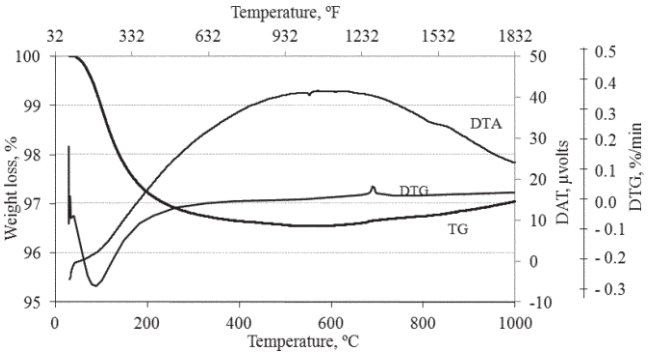

Fig. 11—TG curve of ARPC.

TG analysis.[29] DTG improves the resolution of complex or overlapping TG curves, thus providing additional information about decomposition or mass loss phenomena.[30] The weight loss between 20°C (68°F) and the temperature of the first DTG peak was due to loss of water not chemically bound in hydrates (free water). For temperatures higher than that of the first DTG peak, water losses are due to structural water (dehydration of CSH and dehydroxylation of portlandite) according to Cheyrezy et al.[31] The DTG peak for CRPC between 420 and 500°C (788 and 932°F) was identified as the dehydroxylation of portlandite $Ca(OH)_2$. The peak between 600 and 650°C (1112 and 1202°F) may be due to the dehydration of tobermorite, and the peak at approximately 800°C (1472°F) can be attributed to the decarbonation of calcite. Any instantaneous mass loss in the TG curve was not observed for ARPC and a weight gain occurred beyond 600°C (1112°F). This minor increase may be attributed to the nitriding of some components. The small endotherm in the DTA curves of ARPC and CRPC between 560 to 575°C (1040 to 1067°F) is due to the crystalline inversion of quartz aggregate.

It is reported that relatively small pores (<50 nm) in hardened cementitious systems are commonly attributed to gel pores and micropores, which do not adversely affect the mechanical strength.[21] Uzal et al.[32] showed that a higher volume of pores larger than 100 nm in size adversely affect the mechanical strengths of hardened cementitious pastes. Jiang and Guan[33] also stated that the effect of porosity located in pores with radii $r > 100$ nm is distinctly greater than of those located in pores with other radii. The pore-size distributions of CRPC at 20 and 300°C (68 and 572°F) are given in Fig. 12. As shown in Fig. 12, the amount of mesopores (pore diameter between 2.5 and 50 nm) was increased significantly parallel to the increase of temperature from 20 to 300°C (68 to 572°F). However, change was not observed in the amount of pores that have a diameter greater than 100 nm. It is known that pores that have a diameter greater than 100 nm are responsible for the strength of the binder. This explains why the compressive strength of CRPC exposed to 300°C (572°F) did not decrease compared to 20°C (68°F).

The pore-size distributions of ARPC at 20, 200, and 600°C (68, 392, and 1112°F) are given in Fig. 13. As shown in Fig. 13, the temperature increase resulted in a coarser pore-size distribution for ARPC in both macro- and mesopores. The strength reduction for ARPC can be related to the increase of pore size.

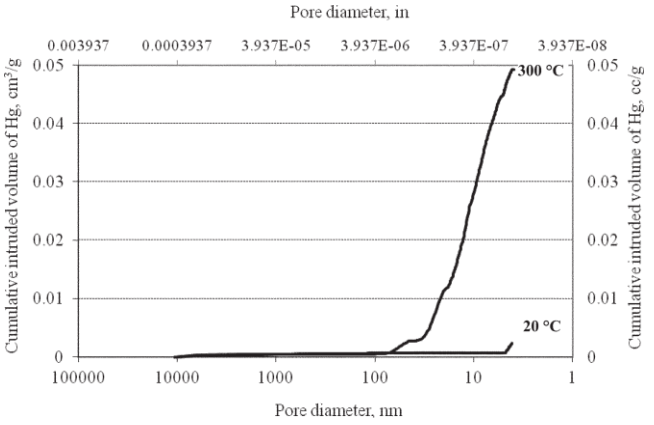

Fig. 12—Pore-size distributions of CRPC for 20 and 300°C (68 and 572°F).

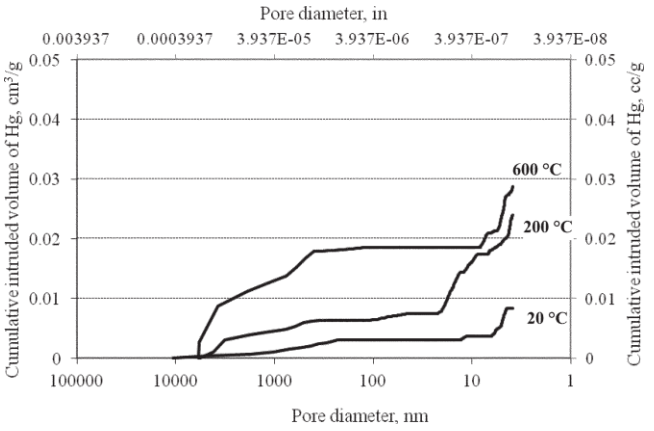

Fig. 13—Pore-size distribution of ARPC for 20, 200, and 600°C (68, 392, and 1112°F).

CONCLUSIONS

Based on the results of this experimental investigation, the following conclusions are drawn:

1. CRPC has a superior high temperature resistance up to 300°C (572°F) without any strength and toughness loss. However, from 400°C (752°F) and up, this composite suffers explosive spalling. In other words, beyond 400°C (752°F), the integrity and load-bearing capacity of the element may be jeopardized and leads to complete destruction of the structure. The temperature in many fires significantly exceeds this value in many cases. Thus, CRPC is not an appropriate material for the structures with a high risk of fire.

2. Microstructural formations result in a major difference in the high temperature behaviors of CRPCs and ARPCs. ARPC does not suffer explosive spalling due to its nano-sized pored microstructure. These pores permit the quick escape of water vapor from the ARPC matrix, resulting in lower internal pore pressures.

3. The mechanical properties of ARPC decreased gradually with the increase of temperature. Furthermore, this composite showed a significant volume change at approximately 800°C (1472°F). However, the residual mechanical properties are still considerably high enough to prevent total collapse of the structure.

4. The suggested SF limits by various researchers for HPC to avoid explosive spalling are not valid for ARPC. Although this composite includes 20% of SF, none of these specimens exploded, even at the high rates of heating (25°C/minute [77°F/minute]) up to 800°C (1112°F).

5. In conclusion, it can be said that ARPC seems to be a promising high-performance material for structures with a high fire risk due to its nonexplosive spalling behavior.

REFERENCES

1. Aydın, S.; Yazıcı, H.; and Baradan, B., "High Temperature Resistance of Normal Strength and Autoclaved High Strength Mortars Incorporated Polypropylene and Steel Fibers," *Construction & Building Materials*, V. 22, 2008, pp. 504-512.

2. Chan, S. Y. N.; Luo, X.; and Sun, W., "Effect of High Temperature and Cooling Regimes on the Compressive Strength and Pore Properties of High Performance Concrete," *Construction & Building Materials*, V. 14, No. 5, 2000, pp. 261-266.

3. Kalifa, P.; Menneteau, F. D.; and Quenard, D., "Spalling and Pore Pressure in HPC at High Temperatures," *Cement and Concrete Research*, V. 30, 2000, pp. 1915-1927.

4. Aitcin, P. C., "The Durability Characteristics of High Performance Concrete: A Review," *Cement and Concrete Composites*, V. 25, 2003, pp. 409-420.

5. Chan, Y. N.; Peng, G. F.; and Anson, M., "Residual Strength and Pore Structure of High-Strength Concrete and Normal Strength Concrete after Exposure to High Temperatures," *Cement and Concrete Composites*, V. 21, 1999, pp. 23-27.

6. Poon, C. S.; Azhar, S.; Anson, M.; and Wong, Y. L., "Comparison of the Strength and Durability Performance of Normal and High-Strength Pozzolanic Concretes at Elevated Temperatures," *Cement and Concrete Research*, V. 31, 2001, pp. 1291-1300.

7. Hertz, K. D., "Limits of Spalling of Fire-Exposed Concrete," *Fire Safety Journal*, V. 38, 2003, pp. 103-116.

8. Bonneau, O.; Vernet, C.; Moranville, M.; and Aitcin, P. C., "Characterization of the Granular Packing and Percolation Threshold of Reactive Powder Concrete," *Cement and Concrete Research*, V. 30, 2000, pp. 1861-1867.

9. Richard, P., and Cheyrezy, M., "Composition of Reactive Powder Concretes," *Cement and Concrete Research*, V. 25, 1995, pp. 1501-1511.

10. Richard, P., and Cheyrezy, M. H., "Reactive Powder Concretes with High Ductility and 200-800 MPa Compressive Strength," *Concrete Technology Past, Present, and Future—Proceedings of the V. Mohan Malhotra Symposium*, SP-144, P. K. Mehta, ed., American Concrete Institute, Farmington Hills, MI, 1994, pp. 507-518.

11. Aydın, S., "Development of a Fiber Reinforced Composite with Alkali Activated Ground Granulated Blast Furnace Slag," PhD thesis, Dokuz Eylul University, Izmir, Turkey, 2010, 317 pp.